Atmos. Chem. Phys., 16, 15451–15460, 2016
www.atmos-chem-phys.net/16/15451/2016/
doi:10.5194/acp-16-15451-2016

Atmospheric Chemistry and Physics Open Access EGU

Investigating the impact of regional transport on $PM_{2.5}$ formation using vertical observation during APEC 2014 Summit in Beijing

Yang Hua[1,2], Shuxiao Wang[1,2], Jiandong Wang[1,2], Jingkun Jiang[1,2], Tianshu Zhang[3], Yu Song[4], Ling Kang[4], Wei Zhou[1,2], Runlong Cai[1,2], Di Wu[1,2], Siwei Fan[1,2], Tong Wang[1,2], Xiaoqing Tang[5], Qiang Wei[6], Feng Sun[6], and Zhimei Xiao[7]

[1]State Key Joint Laboratory of Environment Simulation and Pollution Control, School of Environment, Tsinghua University, Beijing 100084, China
[2]State Environmental Protection Key Laboratory of Sources and Control of Air Pollution Complex, Beijing 100084, China
[3]Anhui Institute of Optics and Fine Mechanics, Chinese Academy of Sciences, Hefei 230031, China
[4]College of Environmental Sciences and Engineering, Peking University, Beijing, 100871, China
[5]Hebei Environmental Monitoring Center, Hebei 050051, China
[6]Beijing Environmental Monitoring Center, Beijing 100048, China
[7]Tianjin Environmental Monitoring Center, Tianjin 300191, China

Correspondence to: Shuxiao Wang (shxwang@tsinghua.edu.cn)

Received: 17 August 2016 – Published in Atmos. Chem. Phys. Discuss.: 5 September 2016
Revised: 13 November 2016 – Accepted: 17 November 2016 – Published: 15 December 2016

Abstract. During the APEC (Asia-Pacific Economic Cooperation) Economic Leaders' 2014 Summit in Beijing, strict regional air emission controls were implemented, providing a unique opportunity to investigate the transport and formation mechanism of fine particulate matter ($PM_{2.5}$). This study explores the use of vertical observation methods to investigate the influence of regional transport on $PM_{2.5}$ pollution in Beijing before and during the APEC Summit. Vertical profiles of extinction coefficient, wind, temperature and relative humidity were monitored at a rural site on the border of Beijing and Hebei Province. Three $PM_{2.5}$ pollution episodes were analyzed. In episode 1 (27 October to 1 November), regional transport accompanied by the accumulation of pollutants under unfavorable meteorological conditions led to the pollution. In episode 2 (2–5 November), pollutants left from episode 1 were retained in the boundary layer of the region for 2 days and then settled down to the surface, leading to an explosive increase of $PM_{2.5}$. The regional transport of aged aerosols played a crucial role in the heavy $PM_{2.5}$ pollution. In episode 3 (6–11 November), emissions from large point sources had been controlled for several days while primary emissions from diesel vehicles might have led to the pollution. It is found that ground-level observation of meteorological conditions and air quality could not fully explain the pollution process, while vertical parameters (aerosol optical properties, winds, relative humidity and temperature) improved the understanding of regional transport influence on heavy pollution processes. Future studies may consider including vertical observations to aid investigation of pollutant transport, especially during episodic events of rapidly increasing concentrations.

1 Introduction

With rapid economic development and increases in energy consumption, a large quantity of emissions has caused serious particulate matter pollution in China. Monitoring data shows that the Beijing–Tianjin–Hebei (BTH) region is one of the most polluted regions in China (B. Zhao et al., 2013; Wang et al., 2014). The region was home to 8 of the 10 most polluted Chinese cities in 2014 according to the reports published by Ministry of Environment Protection (MEP, 2015). In 2014, the annual average $PM_{2.5}$ (particulate matter with aerodynamic diameter less than 2.5 µm) concentration reached 95 µg m^{-3} in the BTH region. With 21.5 million residents and 5.3 million vehicles in 2014, Beijing has frequently been burdened with severe pollution episodes in

recent years (Beijing Municipal Bureau of Statistics, 2015). The capital is surrounded by mountains in three directions (north, west and east). The top three most polluted cities in China (Baoding, Xingtai and Shijiazhuang) are located south of Beijing. Polluted air masses from the south contribute to $PM_{2.5}$ pollution in Beijing (Wang et al., 2015). Source apportionment by the Beijing Environmental Protection Bureau indicates that regional transport contributed 28–36 % to $PM_{2.5}$ in Beijing in 2012–2013. During some severe pollution periods, regional contribution was more than 50 % (http://www.bjepb.gov.cn/bjepb/413526/331443/331937/333896/396191/index.html). Quite a few studies have researched the causes of heavy pollution episodes in the BTH region, and they show that regional transport plays an important role in pollution formation. The sharp $PM_{2.5}$ buildup events in Beijing were unique, while pollution accumulated more slowly in other cities in the region. This indicated that $PM_{2.5}$ was probably transported to Beijing from other cities (Zheng et al., 2015; Ji et al., 2014; Tao et al., 2014; X. J. Zhao et al., 2013). Meanwhile, most severe pollution occurs under stable synoptic meteorological conditions in Beijing (Sun et al., 2015; Zheng et al., 2015; X. J. Zhao et al., 2013). The low wind speed and stable synoptic meteorological conditions at ground level cannot explain the reason why regional transport contributes significantly to severe pollution. A previous study showed that the secondary aerosol in Beijing probably mainly forms over regional transport, according to a vertical observation from the ground to 260 m height (Sun et al., 2015). Therefore, vertical profiles of meteorology and air quality might help us to understand the impacts of regional transport on heavy pollution during stagnant conditions.

As in other megacities with local sources and regional transport, air quality in Beijing is affected by many factors, including emissions inside the city, formation of secondary pollutants, atmospheric mixing and regional transport. It is well known that the strength of each factor varies according to emissions and/or weather conditions. Therefore, it is challenging to pinpoint the major contributors to clean or polluted episodes in any given time period. This is especially difficult in the BTH region, considering the complicated emission sources and transport processes.

Emission control measures implemented during some events provide a unique opportunity to investigate the impact of various factors that influence air quality. One of them was the APEC (Asia-Pacific Economic Cooperation) Economic Leaders' 2014 Summit held in Beijing from 5 to 11 November 2014. A strict emission pollution control plan was carried out in the BTH region to improve air quality in Beijing from 3 to 11 November for APEC. According to a conservative estimate by MEP, production of 9289 plants was paused and 3900 plants were running at reduced capacity in six provinces (Beijing, Tianjin, Hebei, Shanxi, Shandong and Inner Mongolia), and more than 40 thousand construction sites were shut down temporarily (http://www.zhb.gov.cn/gkml/hbb/qt/201411/t20141115_291482.htm). Other measures included traffic control (50 % of private passenger vehicles and 70 % of buses were off-road) and frequent road sweeping and cleaning in Beijing. More detailed emission control measures are supplied in the Supplement. Studies found that regional emission control effectively reduced air pollutant concentrations during the summit (Wen et al., 2015; Tang et al., 2015; Han et al., 2015; C. Chen et al., 2015; Sun et al., 2016a). The significantly reduced local emissions led to reduced complexity of particulate matter pollution processes, thus providing a unique opportunity to investigate the influence of transport events on $PM_{2.5}$ levels in Beijing.

The objective of the study is to investigate the impact of regional transport on $PM_{2.5}$ in Beijing using both ground-level and vertical observations. Field observation was conducted at a rural site (Liulihe) southwest of Beijing before and during the control period of the APEC 2014 Summit. Vertical profiles of temperature, RH (relative humidity), wind speed and direction, and extinction coefficient were observed as well as pollutant concentration and meteorological parameters on the ground. The characteristics of three $PM_{2.5}$ pollution episodes were analyzed. Findings of this study will help explore vertical observation methods for in-depth analysis of meteorological and transport influence. Furthermore, these findings can aid the development of future air quality management strategies in BTH and other regions around the globe, including emission control and air surveillance.

2 Field observation and analysis methods

2.1 Field observation site and sampling methods

Beijing is surrounded by mountains in the west, north and east, which blocks pollutants from spreading. The open air corridor in the south exposes the capital to air masses that are passing Hebei Province (Fig. S1 in the Supplement), a heavily polluted area in China. To investigate the impact of regional transport on Beijing, a rural site (Liulihe site, 116°2′ E, 39°36′ N) southwest of Beijing was chosen. It was located on the border of Beijing and Hebei Province (Fig. S1).

The field campaign was conducted from 27 October to 12 November 2014, including both ground-level and vertical observations. All the times discussed in this article are Local Time. Detailed information of instruments at the Liulihe site is provided in Table S1. Ground-level observations included meteorological parameters, mass concentration of $PM_{2.5}$/PM_{10}, SO_2, NO_x and O_3 as well as physical and chemical properties of PM. $PM_{2.5}$–PM_{10} mass concentration was determined by the tapered element oscillating microbalance (TEOM) method. Particle size distribution from 3 nm to 10 µm was measured by a spectrometer assembled in-house, including one nano scanning mobility particle sizer

(NSMPS), one scanning mobility particle sizer (SMPS), and one aerodynamic particle sizer (APS) (Liu et al., 2014).

ACSM (Aerosol Chemical Speciation Monitor), a low-maintenance aerosol mass spectrometer, was used to measure non-refractory (NR) particulate matter with aerodynamic diameters smaller than 1 μm (PM_1) (Ng et al., 2011). The ACSM data were calibrated with a collection efficiency (CE) value to compensate for the particle loss. The CE value of 0.45 recommended by Middlebrook et al. (2012) based on the monitoring site condition (see Supplement) was used in this study. The NR-PM_1 concentration measured by ACSM tracks well with $PM_{2.5}$ measured by the TEOM ($R^2 = 0.91$), and the regression slope is 0.43 (Fig. S2). Positive matrix factorization (PMF) with the PMF2.exe algorithm was used to distinguish different components of OA measured by ACSM (Paatero and Tapper, 1994). The PMF was performed and evaluated following the PMF analysis guide (http://cires1.colorado.edu/jimenez-group/wiki/index.php/PMF-AMS_Analysis_Guide). Three factors were distinguished (Fig. S3), i.e., HOA (hydrocarbon-like organic aerosol), SVOOA (semi-volatile oxygenated organic aerosol) and LVOOA (low-volatile oxygenated organic aerosol).

Beyond ground-level concentrations of routinely monitored air pollutants and meteorological parameters, the assessment was aided by vertical observations, including vertical extinction coefficient profiles as well as vertical wind, RH and temperature profiles. The vertical extinction coefficient profiles depict the distribution of PM, which could be used to infer the mixing process of particles transported from high evaluations and those near the ground. Vertical wind profiles indicate the transport direction. Vertical RH profiles reflect the strength of heterogeneous reaction at different layers. Vertical temperature profiles provide information on the stability of and mixing in the boundary layer. Lidar was used to observe the vertical optical properties of atmospheric aerosols at the Liulihe site. The lidar consisted of three parts, including emitting system, receiving system and signal analogue system (Z. Chen et al., 2015). The laser source emitted a pulse at 355/532 nm. The pulse energy was 30 MJ at 355 nm and 20 MJ at 532 nm. The pulse repetition was 20 Hz. The telescope for the receiving system was based on a Cassegrain design. Diameter of the telescope was 200 mm with a vertical resolution of 7.5 m. The particle backscatter coefficient and extinction coefficient was retrieved using the Fernald method (Fernald, 1984). CFL-03 phased array wind profile radar was used to monitor the vertical wind speed and direction with resolutions of 50 m (0–1 km) and 100 m (1–5.5 km). Parameters of these instruments can be found in another paper (Wang et al., 2013). There was a 300 m blind area for CFL-03. Vertical profiles of atmospheric temperature and humidity were derived by profiling radiometers. The channel center frequencies were 22–32 GHz (K band) and 51–59 GHz (V-Band). The vertical resolutions were 60 m (0–4 km) and 120 m (4–10 km).

2.2 Back-trajectory analysis

TrajStat, a GIS-based software into which the HYSPLIT (Hybrid Single Particle Lagrangian Integrated Trajectory) model was loaded (Wang et al., 2009), was used to calculate the back-trajectory. The model was run every 6 h in a 24 h mode back-trajectory mode at 1000 m above sea level from the Liulihe site to identify the origins and pathways of air mass. The meteorology data used in the mode were obtained from the Global Data Assimilation System (GDAS) model (http://www.ready.noaa.gov/READYamet.php).

2.3 Quantification of regional transport contribution

A novel technique was used to quantify the contribution of regional transport (Jia et al., 2008). The diurnal trend of $PM_{2.5}$ in Beijing often exhibits "saw-tooth cycles" with a smoothly increasing or decreasing baseline upon which daily cycles are superimposed. Ancillary measurements around Beijing show that the baselines represent regional aerosols, while the daily cycles represent local aerosols. Following Jia et al. (2008), the total contribution is defined as the area under the concentration line (A_t), while its regional component is defined as the area under the baseline curve (A_r). Both areas are approximated using trapezoid numerical integration as Eq. (1):

$$A_N = \sum_{n=1}^{N-1} A_i = \sum_{n=1}^{N-1} \frac{(C_i + C_{i+1})}{2} \times (t_{i+1} - t_i), \quad (1)$$

where N is the total number of hourly $PM_{2.5}$ concentrations in a specific time period, C_i is the total concentration (for A_t) or baseline concentration (for A_r) value at time t_i ($i = 1, N-1$). The baseline concentration curve is the line connecting daily afternoon minimal values. The percentage regional contribution (R) is expressed as the following Eq. (2):

$$R = \frac{A_r}{A_t} \times 100\,\%. \quad (2)$$

The uncertainty evaluation mainly includes systematic errors, random errors and sensitivities. The major systematic errors depend on the calibration of instruments for $PM_{2.5}$ concentration measurement. Minor systematic errors might come from judging the location and height of the daily minima, and the sensitivity analysis suggests that these errors are less than 10 %. Random errors include data measurement and quantification steps, such as identifying the daily minima properly, dealing with days without less obvious afternoon minima and using linear interpolation between the daily minima. All these errors were evaluated by Jia et al. (2008). As a whole, this technique has an uncertainty of 40–50 % for the results of daily regional transport.

3 Results and discussion

3.1 General characteristics of atmospheric pollution before and during the APEC Summit

To investigate the changes in air quality during the APEC Summit, average pollutant concentrations and the rates of change were calculated. Concentrations of $PM_{2.5}$, SO_2 and NO_2 decreased significantly during the emission control (3–12 November) compared to the period before control (27 October to 2 November), shown in Fig. S4a. Large rates of reduction were observed for NO_2 (37 %) and SO_2 (36 %), while the reduction in $PM_{2.5}$ was smaller (21 %) but still significant (Fig. S4b).

Three pollution episodes were selected to discuss the pollution characteristics during the observation (Fig. S5). Episode 1 (27 October to 1 November) represents the period before the emission control. Episode 2 (2–5 November) was the first pollution episode during the emission control. Episode 3 (6–11 November) was the second pollution episode during the emission control. $PM_{2.5}$ concentration at the Miyun site (located in northern Beijing, shown in Fig. S1, data source: Beijing EPB) is shown in Fig. S5 alongside Liulihe to demonstrate the synchronism of $PM_{2.5}$ levels at different sides in Beijing. At Liulihe, $PM_{2.5}$ concentration was the highest in episode 1 ($140 \pm 70\,\mu g\,m^{-3}$) before implementation of emission control, whereas the mean values were close during the last two episodes (91 ± 75 and $89 \pm 61\,\mu g\,m^{-3}$).

The average concentration of online non-refractory PM_1 chemical components was shown in Fig. 1. Average concentrations of OM (organic matter), NH_4^+, SO_4^{2-} and NO_3^- were the highest in episode 1 before emission control. During episode 2, those compounds decreased by 32–60 %. In episode 3, the average concentrations remained similar except for NH_4^+, which decreased by 12 %. HOA (related to primary emission), LVOOA and SVOOA were distinguished. Compared with episode 1, HOA, LVOOA and SVOOA decreased by 22, 58 and 28 %, respectively, in episode 2. After that, LVOOA kept decreasing by 10 % in episode 3, while HOA and SVOOA increased by 39 and 5 %.

Overall, most meteorological parameters changed little during the three episodes except for RH (Fig. S6). The average ground-level RH (69 %) in episode 1 was higher compared with those in episode 2 (50 %) and in episode 3 (58 %). Wind speed remained low during the entire observation. The average wind speed was 0.5, 0.8 and $0.7\,m\,s^{-1}$ in episode 1, episode 2 and episode 3, respectively. The dominant wind direction was southwest during the 17 days of observation. The frequency of southwestern wind was above 60 % during each of the three episodes, with the highest occurrence of 81 % observed during episode 2.

The significant reduction in pollutant concentrations during APEC implies that the emission control was effective. However, the general characteristics derived from ground-level observation are insufficient to identify the leading cause of particulate matter pollution, local emissions, regional transport or both. Furthermore, the significant differences in particle chemical component changes from episode 2 to episode 3 under similar ground-level meteorological conditions and local emission intensity suggest different transport or formation mechanisms during those two episodes. Therefore, vertical observations will be used to aid further investigation in each of the three episodes in the following section.

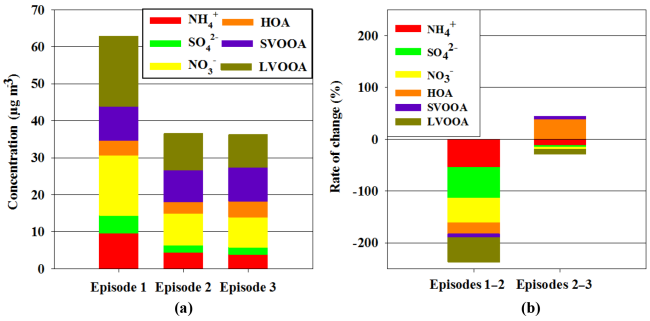

Figure 1. Non-refractory PM_1 chemical components at the Liulihe site during the three episodes. **(a)** Average non-refractory PM_1 chemical components, **(b)** differences of chemical components among episodes.

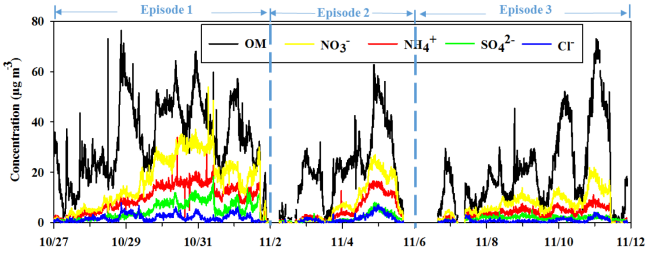

Figure 2. Temporal changes of non-refractory PM_1 chemical components at the Liulihe site.

3.2 Characteristics of heavy $PM_{2.5}$ pollution episodes and contribution of regional transport

3.2.1 Pollution process in episode 1

Episode 1 (27 October to 1 November) was before emission control. The average concentration of $PM_{2.5}$ reached $140 \pm 70\,\mu g\,m^{-3}$. This high level of $PM_{2.5}$ is typical in Beijing during autumn. There were two unique features in this episode. One is the continued increase of $PM_{2.5}$ mass and PM_1 component concentrations during the first 4 days, with OM showing a more distinct diurnal cycle (Figs. 2, 3 and S5). Another is the rapid increase of OM on 29 October (Fig. 3). Both suggest that other mechanisms, except for secondary formation, might impact the OM growth and need further investigation.

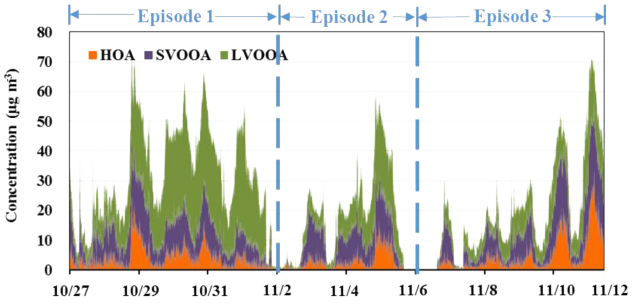

Figure 3. The temporal changes of organic components in PM_1 at the Liulihe site.

Various parameters collected during episode 1 are shown in Fig. 4. Combining the ground-level observation and vertical observation, it is evidenced that the pollution was caused by regional transport and later pollutant accumulation. Vertical extinction coefficient data observed at the Yongledian site (116°47′ E, 39°43′ N) near the Liulihe site were used (Fig. 4a) because the optical lidar at Liulihe did not work in October. High levels of PM appeared at approximately 2 km above ground (Fig. 4a) and remained there for 1 day. The air mass came from the southwest, where emissions were high (see horizontal wind direction profile, Fig. 4c). Back-trajectories also show air masses from the southwest arriving in Liulihe as well as Yongledian (Fig. S7). Then pollutants settled down (see downward vertical wind direction in Fig. 4b) and mixed with aerosols on the ground (Fig. 4a). The online particle size distribution also implied transport processes. During the same period (from 13:00 to 20:00 LT on 28 October), a new group of particles appeared and mixed with existing particles, indicating the arrival of aged aerosols (Fig. 4e). As mentioned above, except for secondary formation, other mechanisms might impact OM increase. The increase of OM might come from freshly emitted organic particles that are transported to the site instead of aged particles. One piece of evidence is that both HOA and OOA increased significantly. Another is that the OM peak appeared after the transport occurrence, much earlier than SNA. Notice that even though wind direction on the ground changed to north early in the morning on 29 October, it still remained from the southwest above 500 m, indicating significant influence of regional transport.

In the next 2 days (30–31 October), vertical wind direction was downward, which was unfavorable for pollutant diffusion (Fig. 5a). Weather Research & Forecasting Model (WRF) modeling results also showed that the whole region was under the control of weak downward wind from late on the night of 30 October (Fig. S8, modeling parameters are provided in the Supplement). Furthermore, both the atmosphere press and wind speed decreased at the same time (Fig. S6). This indicates that the site was probably in the rear of a cold anticyclone. The steady weather conditions promoted pollutant accumulation. Meanwhile, high RH on the surface (Fig. S6) enhanced the formation of SA (secondary aerosol), as pointed out by Pathak et al. (2009). Under this condition, NH_4^+, SO_4^{2-} and NO_3^- concentrations increased at rates of 0.26, 0.21 and 0.58 $\mu g\,m^{-3}\,h^{-1}$, respectively. The peak of NH_4^+, SO_4^{2-} and NO_3^- concentrations was 2 days later than OM. This also proved that the organic particles were transported to Beijing and reached the peak on 29 October and that secondary formation became severe later, both of which promoted the pollution occurrence.

To quantify the impact of regional transport, the transport component is calculated with the method introduced in Sect. 2.2. The baseline needs to be defined first, especially for pollution end timing. The vertical observation and ground observation were combined to discuss when the pollution ended (see Supplement). The regional component is calculated based on the determination of the baseline. For episode 1, the regional component accounted for 75 % of $PM_{2.5}$ mass concentration observed at the Liulihe site, indicating the important influence of regional transport on the pollution. It can be seen that episode 1 was a pollution episode influenced by transport processes in Beijing. RH was high, wind speed was continuously low and wind direction was mainly from the southwest on the surface. Vertical observation showed that the pollutants transported from the southwest settled down. OM concentration increased significantly when the transport PM was observed. After that the low wind speed and high RH easily promoted pollutant accumulation, and downward vertical wind was unfavorable for pollutant diffusion.

3.2.2 Pollution process in episode 2

Episode 2 (2–5 November) saw a lower mean $PM_{2.5}$ concentration ($91 \pm 75\,\mu g\,m^{-3}$) due to the implementation of emission control since 2 November. Unlike the gradual accumulation of PM observed in episode 1, $PM_{2.5}$, OM and SNA had a sharp increase from 4–5 November. The concentrations of NH_4^+, SO_4^{2-} and NO_3^- increased at rates from the lowest to the highest of 0.88, 0.43 and 1.64 $\mu g\,m^{-3}\,h^{-1}$, respectively, much faster than the rates in episode 1. OOA also increased much more significantly during this episode. The explosive increases of PM components, mainly SA, in such a short period of time is contrary to lower RH values in this episode, leading to a less heterogeneous reaction. Thus, such rapid increases in PM levels could be due to the transport of aged aerosol from other regions, as hypothesized by previous studies where the transport process was not directly observed (Yue, et al., 2009; Massling et al., 2009; Sun et al., 2014, 2016b).

With the aid of vertical observation, an in-depth investigation revealed atmospheric processes leading to the peak concentrations during 4–5 November. Firstly, after episode 1 ended on 1 November, relatively high PM levels still resided at 1000 m (from 2 to 3 November), as shown in the vertical extinction coefficient (Fig. 7). Furthermore, a band of

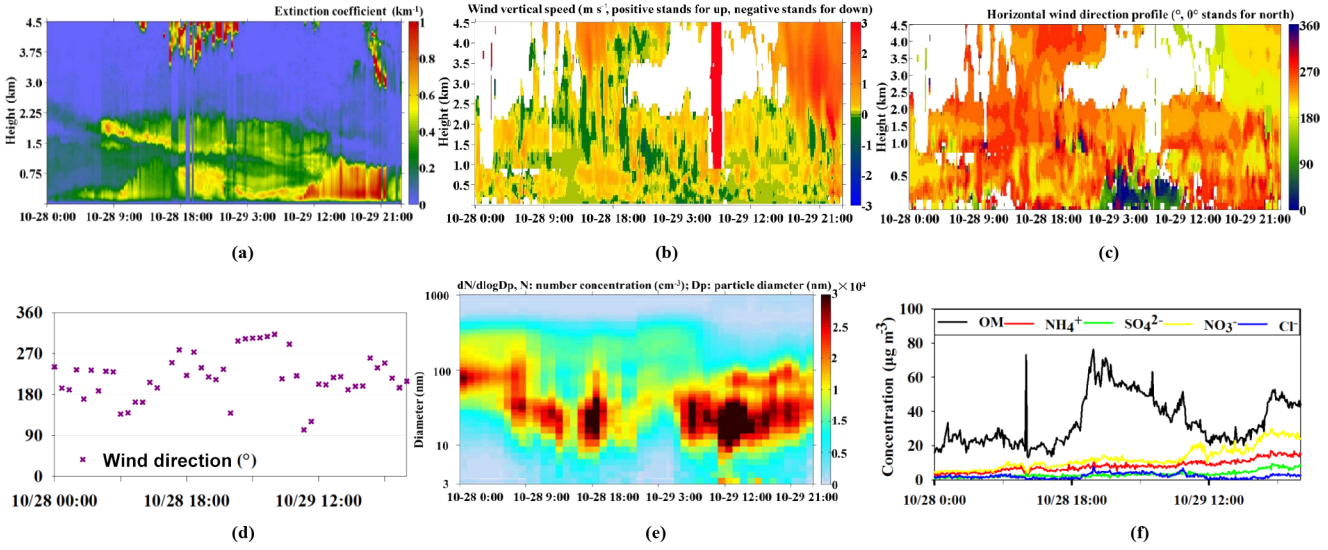

Figure 4. Characteristics of particulate matters and meteorological parameters during episode 1. **(a)** Vertical profile of extinction coefficient (Yongledian site), **(b)** vertical profile of wind vertical direction and speed, **(c)** horizontal wind direction profile, **(d)** wind direction on the ground, **(e)** particle size distribution, **(f)** NR-PM_1 chemical components.

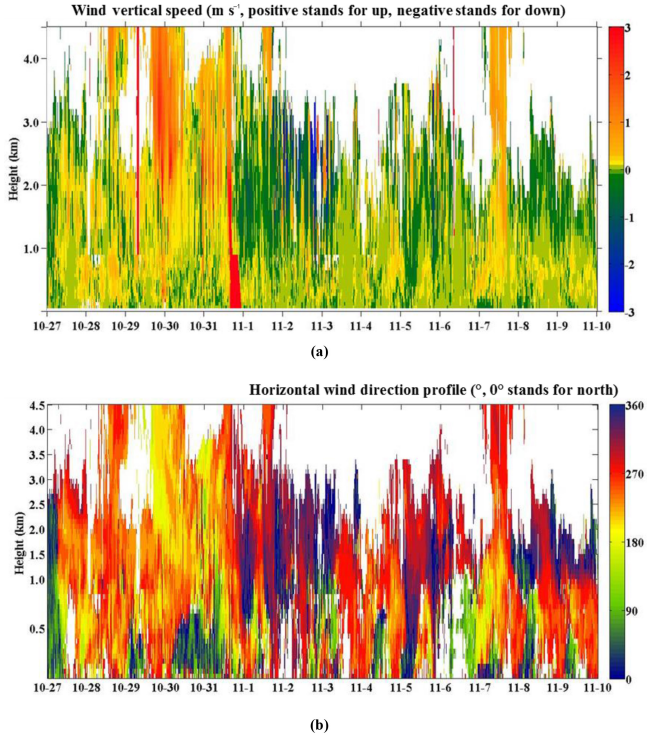

Figure 5. Vertical profile of wind at the Liulihe site. **(a)** Wind vertical speed, **(b)** wind horizontal direction profile.

high PM centered around 750 m was observed (Fig. S9) on 3 November at another site (Baoding site, 115°31′ E, 38°52′ N; shown in Fig. S1) in the BTH region, suggesting a widespread PM aloft in the region. During the next 2 days, the pollutants were transported in the region and the slow winds (average speed of 4.8 m s^{-1} at 1000 m) allowed aerosols ample time to age in their journey. Back-trajectories showed transport of air mass from the southwest on the night of 3 November (Fig. S10), consistent with the vertical wind profile observed at Liulihe (Figs. 5 and 9). On 3 and 4 November, the downward motion of air mass around 1000 m above ground intensified, bringing the aged aerosols down and mixing them with the aerosols on the ground. The well-mixed boundary layer with regard to aerosol is evidenced in Fig. 8 with a fairly uniform distribution from the ground to 900 m. Consequently, secondary chemical component concentrations of PM_1 (Figs. 2 and 3) started ascending at remarkably fast rates.

Dry and clean air mass from the north arrived early in the morning on 5 November. RH started to increase significantly at 10:00 LT and wind speed became higher at 12:00 LT . At the same time, $PM_{2.5}$ concentration started to decrease. Based on the analysis, the pollution episode ended at 12:00 LT . The calculation shows that regional transport contributed 62 %, relatively lower than that during episode 1 (Fig. 6).

Rather than chemically reacting, aged aerosols settled down and contributed significantly to the high $PM_{2.5}$ concentration in episode 2. Vertical observations found that the aged aerosol settled down and caused the explosive increase of SNA in such a short time, which cannot be explained by the ground-level observations. It was also noticed that the high $PM_{2.5}$ level appeared when the emission control just started, which means this episode was partly caused by regional transport before control. Even when local emission control was conducted effectively, the uncontrolled regional

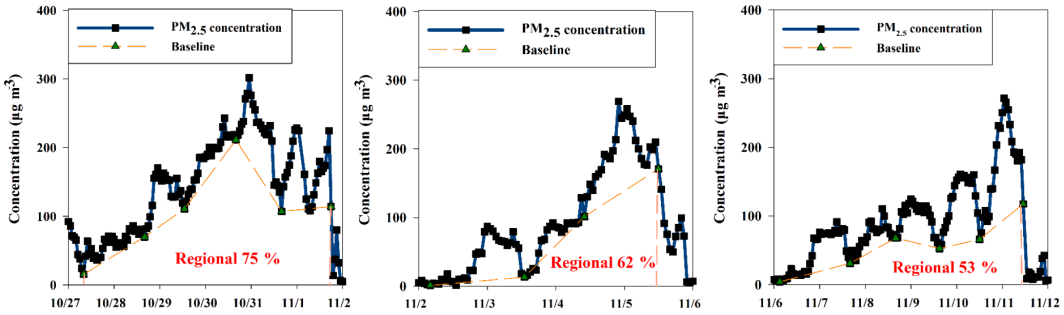

Figure 6. Regional and local components of the three episodes at the Liulihe site.

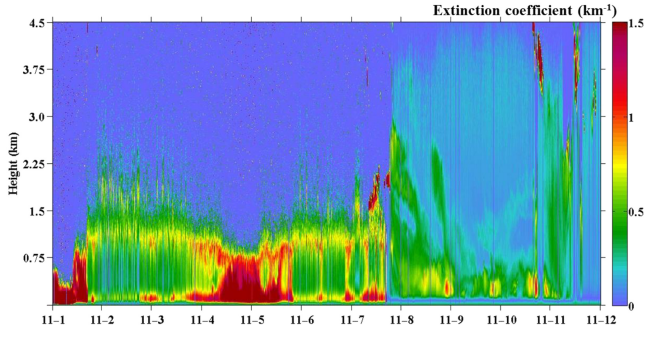

Figure 7. Vertical profile of extinction coefficient at the Liulihe site.

emission still led to severe particulate matter pollution in Beijing.

3.2.3 Pollution process in episode 3

During episode 3 (6–11 November), the Liulihe site recorded a relatively high average $PM_{2.5}$ concentration of $89 \pm 61\,\mu g\,m^{-3}$. Furthermore, this episode is characterized by much more and faster increases in OM concentrations than SNA (Figs. 2 and 3). Specifically, concentrations of aerosol related to fuel combustion (HOA) increased significantly, while SNA increased slowly (NH_4^+ and NO_3^-) or changed little (SO_4^{2-}). All of these indicate that primary emission rather than the formation of SA was the dominant cause.

Vertical extinction coefficient shows that pollutants appeared at 2000–2500 m on 7 November. The air mass came from the northwest and the vertical convection bringing them down on 7 and 8 November (Figs. 7, 5b and 9). Air mass trajectories at 1000 m also show that the air mass arrived in Beijing from the south on 7 November but changed to the northwest on 8 November (Fig. S11). Because of less pollution in the northwest and the effective emission control in the BTH region during the APEC, the regional transport of PM was weakened. This is supported by an estimated regional contribution of 53 % to $PM_{2.5}$ in Beijing, much lower than in episode 1 (75 %) and episode 2 (63 %).

Figure 10 depicts black carbon (BC) concentrations measured by an aethalometer and OM concentrations measured by ACSM. They tracked each other well during this episode. Concentrations of BC, a marker of vehicular emission in urban settings, had two peaks every day. One was early in the morning and another was after morning rush hour around 10:00–11:00 LT . The first peak might have resulted from diesel vehicle emissions (Westerdahl, et al., 2009). This is because transportation of goods to Beijing via heavy-duty diesel vehicles has been permitted at night only, and the number of trucks was large. The second peak might have resulted from vehicles from outside Beijing coming into the city. Vehicles not registered in Beijing are banned from coming into Beijing during the rush hour (07:00 to 09:00 LT), which reduces the morning peaks and smoothes the traffic flow. The vehicles coming into Beijing reach a peak after morning rush hour (http://max.book118.com/html/2016/1022/60419427.shtm). As a result, a second peak appeared late in the morning at the Liulihe site, which is close to the entrance from Hebei Province into Beijing. When the regional emission control was conducted effectively and air mass came from relatively clean areas, traffic emissions in and around the city became the dominant source.

4 Conclusion

This study indicates that sometimes the meteorological conditions on the ground could not explain the air pollution process, especially the air pollution episodes significantly impacted by regional transport of air pollutants. Vertical observation can provide the vertical meteorological and optical profile, which can help identify the regional transport episodes. Combining the ground-level observation with information from radar, we can determine the regional transport influence on air quality.

Three episodes of different types under similar ground meteorological conditions were discussed in this study. In episode 1, particle concentration accumulated under the unfavorable meteorological condition after transport occurred. The transport pollutants later brought organic aerosol and SNA increased under high RH. In episode 2, pollutants left

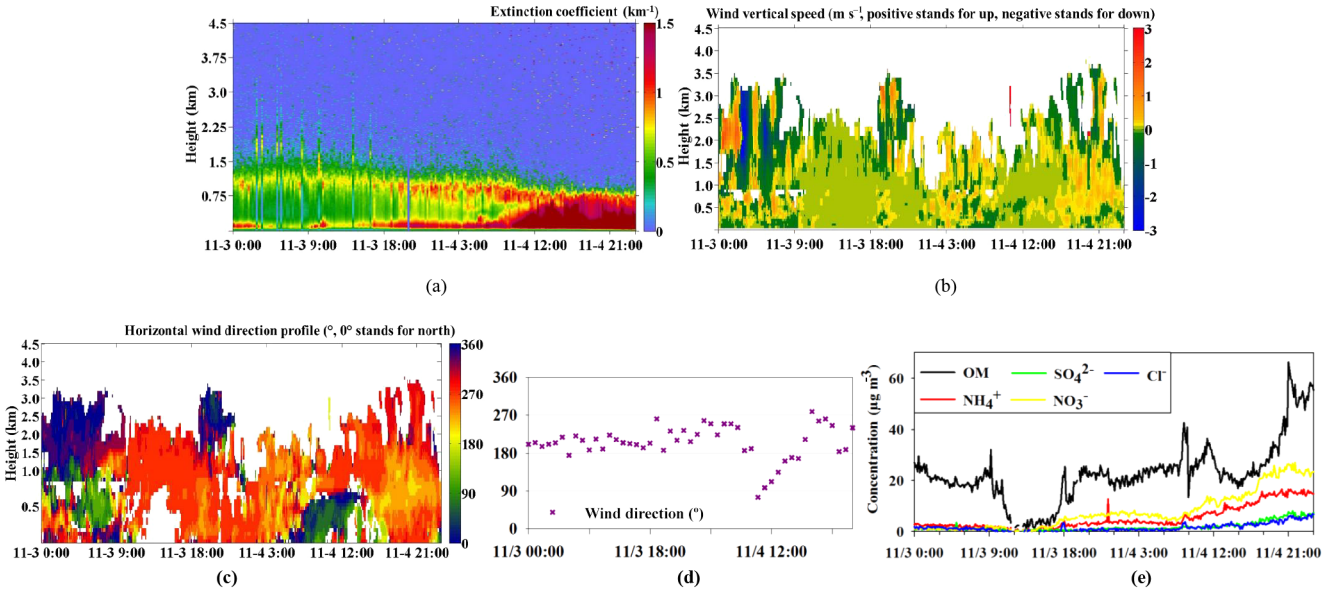

Figure 8. Characteristics of particulate matters and meteorological parameters during episode 2. **(a)** Vertical profile of extinction coefficient, **(b)** vertical profile of wind vertical direction and speed, **(c)** horizontal wind direction profile, **(d)** wind direction on the ground, **(e)** NR-PM_1 chemical components.

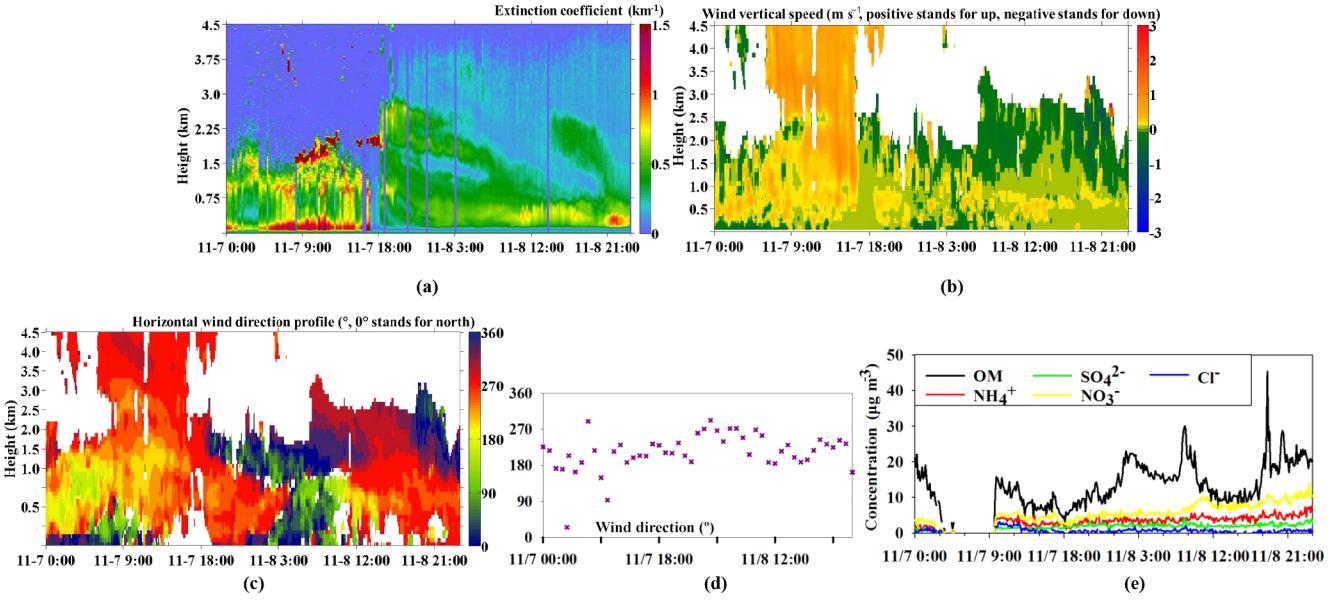

Figure 9. Characteristics of particulate matters and meteorological parameters at the Liulihe site during episode 3. **(a)** Vertical profile of extinction coefficient, **(b)** vertical profile of wind vertical direction and speed, **(c)** horizontal wind direction profile, **(d)** wind direction on the ground, **(e)** NR-PM_1 chemical components.

from episode 1 were retained in the boundary layer in the region. When vertical wind direction changed to downward, the pollutants settled down. As a result, OM and SNA increased explosively. In episode 3, when the control had been conducted for several days, SNA and OA concentration increased much less, while HOA and increased significantly. The pollution might be caused by the primary emission from diesel vehicles.

Our research suggests regional transport of air pollutants has significant contribution (up to 70 %) to severe secondary particle pollution, even when local emission was controlled effectively (53 %, such as during the APEC summit). Although lots of attention was paid to air quality management

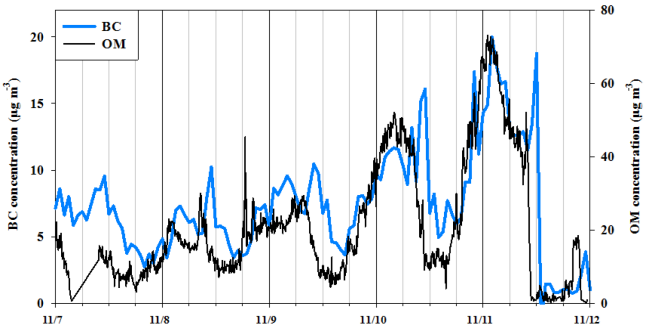

Figure 10. BC and OM concentrations of PM_1 at the Liulihe site during episode 3.

in Beijing, equal efforts need to be paid to regional emission to ensure the clean air. Furthermore, diesel vehicle emission at night in Beijing might be an important pollution source and needs further investigation.

5 Data availability

The data of this paper are available upon request to Shuxiao Wang (shxwang@tsinghua.edu.cn) or Yang Hua (huay09jane@126.com).

The Supplement related to this article is available online at doi:10.5194/acp-16-15451-2016-supplement.

Acknowledgements. This work was supported by the MEP's Special Funds for Research on Public Welfare (201409002), Strategic Priority Research Program of the Chinese Academy of Sciences (XDB05020300), and National Natural Science Foundation of China (21521064 and 21625701). The authors also appreciate the support from the Collaborative Innovation Centre for Regional Environmental Quality.

Edited by: A. Ding
Reviewed by: two anonymous referees

References

Beijing Municipal Bureau of Statistics: The national statistical yearbook of China in 2014, available at: http://data.stats.gov.cn/easyquery.htm?cn=E0103, 2015.

Chen, C., Sun, Y. L., Xu, W. Q., Du, W., Zhou, L. B., Han, T. T., Wang, Q. Q., Fu, P. Q., Wang, Z. F., Gao, Z. Q., Zhang, Q., and Worsnop, D. R.: Characteristics and sources of submicron aerosols above the urban canopy (260 m) in Beijing, China, during the 2014 APEC summit, Atmos. Chem. Phys., 15, 12879–12895, doi:10.5194/acp-15-12879-2015, 2015.

Chen, Z., Zhang, J., Zhang, T., Liu, W., and Liu, J.: Haze observations by simultaneous lidar and WPS in Beijing before and during APEC, 2014, Sci. China Chem., 58, 1385–1392, 2015.

Fernald, F. G.: Analysis of atmospheric lidar observation: some comments, Appl. Optics, 84, 652–653, 1984.

Han, T., Xu, W., Chen, C., Liu, X., Wang, Q., Li, J., Zhao, X., Du, W., Wang, Z., and Sun, Y.: Chemical apportionment of aerosol optical properties during the Asia–Pacific Economic Cooperation (APEC) summit in Beijing, China, J. Geophys. Res.-Atmos., 120, 12281–12295, 2015.

Ji, D., Li, L., Wang, Y., Zhang, J., Cheng, M., Sun, Y., Liu, Z., Wang, L., Tang, G., Hu, B., Chao, N., Wen, T., and Miao, H.: The heaviest particulate air-pollution episodes occurred in northern China in January, 2013: Insights gained from observation, Atmos. Environ., 14, 546–556, 2014.

Jia, Y., Rahn, K. A., He, K., Wen, T., and Wang, Y.: A novel technique for quantifying the regional component of urban aerosol solely from its sawtooth cycles, J. Geophys. Res.-Atmos., 113, doi:10.1029/2008JD010389, 2008.

Liu, J., Jiang, J., Zhang, Q., Deng, J., and Hao, J.: A spectrometer for measuring particle size distributions in the range of 3 nm to 10 µm, Front. Env. Sci. Eng., 16, 63–72, 2014.

Massling, A., Stock, M., Wehner, B., Wu, Z., Hu, M., Brüggemann, E., Gnauk, T., Herrmann, H., and Wiedensohler, A.: Size segregated water uptake of the urban submicrometer aerosol in Beijing, Atmos. Environ., 43, 1578–1589, 2009.

Ministry of Environment Protection (MEP): http://www.zhb.gov.cn/gkml/hbb/qt/201502/t20150202_295333.htm, 2015.

Middlebrook, A. M., Bahreini, R., Jimenez, J. L., and Canagaratna, M. R.: Evaluation of composition-dependent collection efficiencies for the aerodyne aerosol mass spectrometer using field data, Aerosol Sci. Tech., 46, 258–271, 2012.

Ng, N. L., Herndon, S. C., Trimborn, A., Canagaratna, M. R., Croteau, P. L., Onasch, T. B., Sueper, D., Worsnop, D. R., Zhang, Q., Sun, Y. L., and Jayne, J. T.: An Aerosol Chemical Speciation Monitor (ACSM) for Routine Monitoring of the Composition and Mass Concentrations of Ambient Aerosol, Aerosol Sci. Tech., 45, 780–794, 2011.

Paatero, P. and Tapper, U.: Positive matrix factorization: A non-negative factor model with optimal utilization of error estimates of data values, Environmetrics, 5, 111–126, 1994.

Pathak, R. K., Wu, W. S., and Wang, T.: Summertime $PM_{2.5}$ ionic species in four major cities of China: nitrate formation in an ammonia-deficient atmosphere, Atmos. Chem. Phys., 9, 1711–1722, doi:10.5194/acp-9-1711-2009, 2009.

Sun, Y., Jiang, Q., Wang, Z., Fu, P., Li, J., Yang, T., and Yin, Y.: Investigation of the sources and evolution processes of severe haze pollution in Beijing in January 2013, J. Geophys. Res.-Atmos., 119, 4380–4398, 2014.

Sun, Y., Du, W., Wang, Q., Zhang, Q., Chen, C., Chen, Y., Chen, Z., Fu, P., Wang, Z., and Gao, Z.: Real-Time Characterization of Aerosol Particle Composition above the Urban Canopy in Beijing: Insights into the Interactions between the Atmospheric Boundary Layer and Aerosol Chemistry, Environ. Sci. Technol., 49, 11340–11347, 2015.

Sun, Y., Wang, Z., Wild, O., Xu, W., Chen, C., Fu, P., Du, W., Zhou, L., Zhang, Q., and Han, T.: "APEC Blue": Secondary Aerosol Reductions from Emission Controls in Beijing, Sci. Rep., 6, 20668, doi:10.1038/srep20668, 2016a.

Sun, Y., Chen, C., Zhang, Y., Xu, W., Zhou, L., Cheng, X., Zheng, H., Ji, D., Li, J., and Tang, X.: Rapid formation and evolution of an extreme haze episode in Northern China during winter 2015, Sci. Rep., 6, 27151, doi:10.1038/srep27151, 2016b.

Tang, G., Zhu, X., Hu, B., Xin, J., Wang, L., Münkel, C., Mao, G., and Wang, Y.: Impact of emission controls on air quality in Beijing during APEC 2014: lidar ceilometer observations, Atmos. Chem. Phys., 15, 12667–12680, doi:10.5194/acp-15-12667-2015, 2015.

Tao, M., Chen, L., Xiong, X., Zhang, M., Ma, P., Tao, J., and Wang, Z.: Formation process of the widespread extreme haze pollution over northern China in January 2013: Implications for regional air quality and climate, Atmos. Environ., 98, 417–425, 2014.

Wang, J., Wang, S., Jiang, J., Ding, A., Zheng, M., Zhao, B., Wong, D. C., Zhou, W., Zheng, G., and Wang, L.: Impact of aerosol–meteorology interactions on fine particle pollution during China's severe haze episode in January 2013, Environ. Res. Lett., 9, 094002, doi:10.1088/1748-9326/9/9/094002, 2014.

Wang, L., Liu, Z., Sun, Y., Ji, D., and Wang, Y.: Long-range transport and regional sources of $PM_{2.5}$ in Beijing based on long-term observations from 2005 to 2010, Atmos. Res., 157, 37–48, 2015.

Wang, M., Wei, W., Ruan, Z., He, Q., and Ge, R.: Application of wind-profiling radar data to the analysis of dust weather in the Taklimakan Desert, Environ. Monit. Assess., 185, 4819–4834, 2013.

Wang, Y., Zhang, X., and Draxler, R. R.: TrajStat: GIS-based software that uses various trajectory statistical analysis methods to identify potential sources from long-term air pollution measurement data, Environ. Modell. Softw., 24, 938–939, 2009.

Wen, W., Cheng, S., Chen, X., Wang, G., Li, S., Wang, X., and Liu, X.: Impact of emission control on $PM_{2.5}$ and the chemical composition change in Beijing-Tianjin-Hebei during the APEC summit 2014, Environ. Sci. Pollut. R., 23, 4509–4521, 2015.

Westerdahl, D., Wang, X., Pan, X., and Zhang, K. M.: Characterization of on-road vehicle emission factors and microenvironmental air quality in Beijing, China, Atmos. Environ., 43, 697–705, 2009.

Yue, D., Hu, M., Wu, Z., Wang, Z., Guo, S., Wehner, B., Nowak, A., Achtert, P., Wiedensohler, A., and Jung, J.: Characteristics of aerosol size distributions and new particle formation in the summer in Beijing, J. Geophys. Res.-Atmos., 114, doi:10.1029/2008JD010894, 2009.

Zhang, Z. Y., Wong, M. S., and Lee, K. H.: Estimation of potential source regions of $PM_{2.5}$ in Beijing using backward trajectories, Atmos. Pollut. Res., 6, 173–177, 2015.

Zhao, B., Wang, S., Dong, X., Wang, J., Duan, L., Fu, X., Hao, J., and Fu, J.: Environmental effects of the recent emission changes in China: implications for particulate matter pollution and soil acidification, Environ. Res. Lett., 8, 024031, doi:10.1088/1748-9326/8/2/024031, 2013.

Zhao, X. J., Zhao, P. S., Xu, J., Meng,, W., Pu, W. W., Dong, F., He, D., and Shi, Q. F.: Analysis of a winter regional haze event and its formation mechanism in the North China Plain, Atmos. Chem. Phys., 13, 5685–5696, doi:10.5194/acp-13-5685-2013, 2013.

Zheng, G. J., Duan, F. K., Su, H., Ma, Y. L., Cheng, Y., Zheng, B., Zhang, Q., Huang, T., Kimoto, T., Chang, D., Pöschl, U., Cheng, Y. F., and He, K. B.: Exploring the severe winter haze in Beijing: the impact of synoptic weather, regional transport and heterogeneous reactions, Atmos. Chem. Phys., 15, 2969–2983, doi:10.5194/acp-15-2969-2015, 2015.